Hindawi
Geofluids
Volume 2020, Article ID 8837897, 10 pages
https://doi.org/10.1155/2020/8837897

Research Article

Experiments and Modeling on the Influence of Interfacial Tension on Imbibition Height of Low-Permeability Reservoir

Xiaoxia Ren,[1,2] **Aifen Li**,[3] **Piyang Liu**,[1] **and Bingqing He**[3]

[1]*Qingdao Key Laboratory for Geomechanics and Offshore Underground Engineering, School of Science, Qingdao University of Technology, Qingdao 266525, China*
[2]*Shandong Key Laboratory of Oilfield Chemistry, China University of Petroleum (East China), Qingdao 266580, China*
[3]*School of Petroleum Engineering, China University of Petroleum (East China), Qingdao 266580, China*

Correspondence should be addressed to Xiaoxia Ren; renxiaoxia1010@163.com

Received 8 July 2020; Revised 6 August 2020; Accepted 11 August 2020; Published 25 August 2020

Academic Editor: Wei Wei

Low-permeability reservoirs have tiny pores with winding and complicated pore throats. The oil recovery efficiency of low-permeability reservoirs can be enhanced through the displacement of reservoir oil through imbibition. In the present study, experiments were conducted to investigate variations in the imbibition height of hydrophilic and weakly-hydrophilic rock samples under different interfacial tensions. An imbibition model considering imbibition resistance and bending of pore throats was established based on fractal theory. According to the experimental results, variations in the imbibition height of low-permeability rock samples with time can be divided into three stages. In the first stage, the capillary force plays a dominant role, while the viscous force and gravity have very slight effects. The imbibition height first increases rapidly and then levels off to a constant rate. With the increase in interfacial tension, the imbibition rate in the first stage increases, the ultimate imbibition height increases initially and then decreases, and the contribution of the imbibition height in the first stage to the ultimate imbibition height becomes greater. There is an optimal interfacial tension that causes the ultimate imbibition height to reach its maximum. The calculated results obtained from the proposed imbibition model are consistent with the experimental results, indicating that the model can accurately reflect the change in the imbibition height in low-permeability reservoirs in the first stage.

1. Introduction

Abundant oil and gas resources are present in low-permeability reservoir formations, which are widely distributed all over the world. Low-permeability reservoirs have small pore radii, few effective pores, and complicated pore throats with abundant microcracks [1]. It is difficult for traditional water-flooding to displace crude oil from capillary tubes in such a system [2]. Therefore, methods for the efficient development of low-permeability reservoirs have been widely studied in the petroleum industry [3].

Research and practice indicate that the displacement of oil through imbibition can significantly enhance the recovery of fractured reservoirs [4]. Generally, imbibition refers to diffusion under the action of capillary force, as the wetting-phase fluid enters the pore throat of rock spontaneously and displaces the nonwetting-phase fluid in the pore [5]. Studying the imbibition characteristics of low-permeability reservoirs and understanding the mechanisms of imbibition displacement can provide an effective method to enhance the recovery of low-permeability reservoirs.

According to current research findings, the interfacial tension of the fluid has a significant effect on the imbibition. Laboratory studies and field practices have yielded both positive and negative observations. The general principle is that surfactants trigger imbibition by either interfacial tension reduction or wettability alteration [6]. Standnes et al. [7] experimentally compared the oil recovery from oil-wet reservoir cores using different surfactant solutions and found that cationic surfactant C12TAB had high efficiency of imbibition. Alshehri et al. [8] found that a reduction in the interfacial tension can decrease the imbibition resistance of the oil-wet core and improve the imbibition effect. Sun et al. [9] reported that the reduction in interfacial tension could

effectively decrease the work of adhesion, which is conducive to improving recovery through imbibition. Santanna et al. [10] performed static imbibition experiments and found that the imbibition rate and the oil recovery factor were higher when an ionic surfactant was used. It has been reported that the wettability change is the primary cause of improving the imbibition recovery rate using surfactants [11]. Babadagli [12] found that nonionic surfactant solution increased the recovery rate and ultimate recovery of heavy oil in water-wet sandstones. This effect was attributed to the change in wettability due to the addition of surfactant. Sun et al. [9] found that the imbibition effects of hydrophilic and lipophilic cores were both influenced by wettability, and the surfactant has a significant effect on the recovery of the lipophilic core through imbibition. Alvarez and Schechter [13] found that the addition of an appropriate surfactant can improve oil recovery by altering wettability and interfacial tension. Shen et al. [14] studied the surfactant solution imbibition in porous media with subnanometer and nanometer capillaries using a mechanical model, and the simulated calculation showed that the change in wettability contributes more to the imbibition recovery of tight oil than lower interfacial tension. Gao et al. [15] found that the imbibition degree of strong water-wet cores was large when water was used for imbibition. Liu et al. [16] found through experiments that the oil recovery through imbibition is improved as the rock wetness is shifted from oil-wet to water-wet. Saputra et al. [17] performed laboratory-scale imbibition experiments and found that oil recovery is enhanced by the addition of surfactant as a result of wettability alteration, and the reservoir properties have a significant effect on the results of surfactant-assisted spontaneous imbibition. Liu et al. [18] found that the addition of surfactant mainly recovered oils in the macropores, whose surfaces can be easily altered to be water-wet by surfactant, while it had less effect on the recovery of oil in the micropores. Kumar and Mandal [19] found that using surfactant solutions as the imbibing fluid can recover oils from sandstone and carbonate samples, mainly due to the alteration of wettability. However, Keijzer and de Vries [20] held that the addition of surfactants would result in extremely low interfacial tension. Consequently, the capillary force would not be sufficient to drive imbibition, thereby influencing the recovery through imbibition. Tang et al. [21] found that the injected surfactant did not improve the displacement effect through pulse imbibition.

In order to analyze imbibition variations, researchers have also established different imbibition models, among which the Lucas-Washburn (LW) model, Terzaghi imbibition model, and Szekely model are frequently cited [22, 23]. The LW model (Equation (1)) can be used to calculate the relationship between imbibition height and imbibition time. However, in this model, the inertia force and gravity of the fluid during imbibition are ignored, thus affecting the accuracy in practical applications.

$$h = \sqrt{\frac{r\sigma \cos\theta}{2\eta} t}, \tag{1}$$

where h denotes the imbibition height of the fluid in the capillary tubes, m; r denotes the radius of the capillary tube, with the unit of m; σ denotes the interfacial tension of fluid, N/m; θ denotes the wetting angle, degrees; t denotes imbibition time, s; and η denotes fluid viscosity, Pa·s.

Zhmud et al. [24] found that the LW model was not suitable for describing the later stage of imbibition due to the influence of gravity and derived a long term model considering the gravitational acceleration:

$$h = \frac{2\sigma \cos\theta}{\rho g r}\left[1 - e^{-\rho^2 g^2 r^3 / 16\eta\sigma \cos\theta \boxtimes t}\right], \tag{2}$$

where g denotes the gravitational acceleration g (9.8 m/s^2), ρ denotes the fluid density, with the unit of kg/m^3.

Based on the model proposed by Zhmud et al., Fries and Dreyer introduced the Lambert W function into the model and proposed a model with better accuracy [25]:

$$h(t) = \frac{a}{b}\left[1 + W\left(-e^{-1-b^2/a \boxtimes t}\right)\right], \tag{3}$$

where $a = \sigma r \cos\theta/4\eta$, and $b = \rho g r^2/8\eta$.

These imbibition models based on LW model can directly calculate the imbibition height. In order to accurately describe the imbibition process, several studies have been performed to develop other kinds of improved models, which can predict the oil recovery rate or volume by imbibition. Cai et al. [26] derived analytical expressions for calculating the capillary rise of wetting liquid in a single tortuous capillary by introducing the tortuosity and fractal dimension for a tortuous capillary, respectively. After that, Cai et al. [27] discussed the effect of tortuosity on capillary imbibition in wet porous media based on the capillary model and fractal geometry and derived an analytical model for the time exponent for capillary imbibition in terms of fractal dimension for tortuous capillaries. Moreover, Cai et al. [28] proposed an analytical model for calculating the weight of wetting liquid imbibed into the porous media, and the predicting results are in good agreement with available experimental data published in the literature. Li and Zhao [29] derived a mathematical model using pore volume fractal dimension to predict the production rate by imbibition and found that there was almost no effect of wettability on the value of the fractal dimension function. Considering the effect of the high-permeability fracture network in the matrix rock, Andersen et al. [30] developed an imbibition model for oil recovery in fractured reservoirs. Considering the sizes and shapes of pores, the tortuosity of imbibition streamlines, and the initial wetting-phase saturation, Cai et al. [31] developed a more generalized spontaneous imbibition model, which can be used to characterize the imbibition behavior of different porous media. Subsequently, Andersen et al. [32] derived an exponential model for predicting the imbibition profile under the right conditions: disk with constant permeability, core with negligible capillary gradients, and constant capillary-pressure derivative in the saturation interval. Ashraf and Phirani [33] developed a one-dimensional model to

predict the position of the fluid fronts during imbibition in a multilayer porous medium.

In summary, the previous experimental studies on spontaneous imbibition mainly focused on the oil recovery volume and rate of imbibition. There are no unified conclusions regarding the effects of interfacial tension on the imbibition height of low-permeability reservoirs. The imbibition height can also directly indicate the imbibition characteristics and can help to understand the imbibition mechanism and select proper surfactants [34]. Therefore, it needs to be comprehensively studied. Actual low-permeability reservoirs have complicated characteristics [35], and the calculation results given by traditional imbibition models are quite different from the real cases. There is much room for improvement in the current models being applied in the field. Therefore, it is necessary to conduct experimental and modeling studies on the imbibition height to guide the enhanced oil recovery of low-permeability reservoirs.

In this paper, the effect of the interfacial tension of imbibition fluids on the imbibition height of hydrophilic and weakly-hydrophilic low-permeability rocks was experimentally studied. Considering the imbibition resistance and bending of pore throat during imbibition, a prediction model for the imbibition height was established based on fractal theory.

2. Materials and Methods

2.1. Preparation of the Imbibition Solution and Measurement of Physical Properties. To study the influence of interfacial tension and salinity on the imbibition height, NaCl and distilled water were used to prepare brine with various salinities: 0, 2500, 25000, and 70000 mg/L. Surfactant TOF-1 (provided by Changqing Oil Field) was selected for testing. TOF-1 has been widely used in Changqing Oil Field as a commercial cleanup additive for fracturing fluids. It is a liquid product whose main ingredient is a cationic fluorocarbon surfactant. The critical micelle concentration of TOF-1 is 3.5×10^{-2} mol/L. TOF-1 was added to prepare the imbibition solution with various volume fractions: 0.001%, 0.005%, 0.05%, 0.5%, and 5%. Next, the density of imbibition solution was measured using a densimeter, the viscosity was measured using a capillary viscometer, and the interfacial tension was tested using TX-500C Spinning Drop Interface Tensiometer. The contact angle was measured using the contact angle analyzer (Kruss DSA100) according to Standard SY/T 5153-2017 [36].

2.2. Preparation of Rock Samples with Different Wettability and Measurement of Physical Properties. Low-permeability outcrop rocks were cut into several cuboid rock samples with cross-sections of 2.5 cm × 2.5 cm and cylindrical parallel rock samples with diameters of 2.5 cm. The samples were placed into a drying oven overnight. The porosity and permeability of the parallel rock samples were measured using a pulse porometer and pulse permeameter [37]. The porosities of prepared rock samples ranged from 14.2% to 14.5%, with an average of 14.3%. Permeability ranged from 0.170 to 0.175 mD, with an average of 0.172 mD. The maximum and minimum diameters of capillary tube (λ_{max} and λ_{min}), and the equivalent radius of the capillary tube (r_c) were obtained by a high-pressure mercury injection capillary force curve [38].

In this paper, rock samples with different degrees of wettability were used for the experiments. Several of the cut rock samples were calcined at 800°C for 24 h in a muffle furnace and denoted as Group A. The unprocessed rock samples were denoted as Group B. Water-wet indices of the parallel samples in Groups A and B were measured by spontaneous imbibition method according to Standard SY/T5153—2017 "Measurement of reservoir rock wettability" [36]. The water-wet index of the samples in Group A ranged from 0.86 to 0.90, with an average value of 0.883, indicating that they belong to hydrophilic rock samples. The water-wet index of Group B ranged from 0.60 to 0.63, so they can be categorized as weakly hydrophilic rock samples.

2.3. Methods for Imbibition Experiments. Through several exploratory experiments, a direct measurement method for imbibition height was established with the experimental equipment shown in Figure 1. First, the dry rock sample was fixed in the support. To prevent water evaporation from occurring on the surface of the rock samples and affecting the experimental results, each rock sample was coated with a transparent hot-melt adhesive at 230°C before the experiment. After the samples cooled to room temperature, the bottom of the samples was then cut off so that the end of the sample was in direct contact with the imbibition solution. Imbibition solution was poured into a beaker until the surface of the liquid was in contact with the bottom end of the rock sample. This point was considered the beginning of the spontaneous imbibition process. During this spontaneous imbibition process, it was necessary to continuously add imbibition solution into the beaker to ensure that there was a solid-liquid contact surface. The entire process was recorded with a camera, and the imbibition height was analyzed. As the interface of the imbibed and unimbibed regions is usually not a horizontal line, the imbibition height was taken as the average of 3–5 height values.

3. Results and Discussion

3.1. Results on Imbibition Height Tests. At a constant temperature of 26°C, the rock samples of Groups A and B were placed in TOF-1 imbibition solution with different volume fractions, respectively, to analyze the change in imbibition height with time.

3.1.1. Variation in Imbibition Height of Rock Samples in Group a. Figure 2 shows the variations of imbibition height as a function of time for the imbibition solution with the salinity of 0 mg/L (deionized water). The imbibition process can be divided into three stages: Stage I is the initial stage of imbibition, in which imbibition height is positively correlated to time; Stage II is the metaphase of imbibition, in which imbibition height is still positively correlated to time, but the slope in this stage is less than that in the first stage and decreases continuously; in Stage III, imbibition height

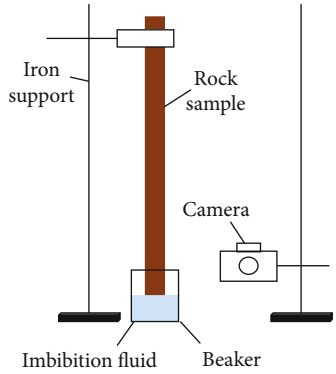

Figure 1: Flow chart of improved imbibition height experiment.

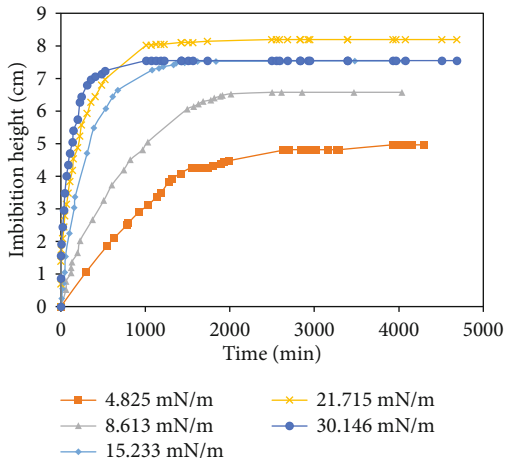

Figure 2: Change in imbibition height with time under different interfacial tensions with a salinity of 0 mg/L.

generally no longer changes, showing that the imbibition has essentially stopped. During the initial stage, the capillary force plays a dominant role and serves as the driving force, while the resistance effect of viscosity and gravity can be neglected [28]. Here, the imbibition height rapidly increases. After the imbibition lasts for several hours, gravity gradually increases, so the imbibition height increases at a lower rate. In the later stage, resistance has a more significant effect, and capillary force as a driving force for imbibition is no longer able to overcome resistance.

The ratio of imbibition height to the duration is defined as the growth rate of imbibition height during the first stage. It is abbreviated as imbibition rate. Table 1 shows the imbibition rates and ultimate imbibition heights under different interfacial tensions with a salinity of 0 mg/L. The imbibition height during Stage I has a higher contribution to the overall imbibition height. Especially under higher interfacial tension (0.001% TOF-1), the imbibition height during Stage I is closer to the ultimate imbibition height. With the increase in interfacial tension, the duration of Stage I reduces, the imbibition height increases, and the imbibition rate accelerates. This is because with the increase in interfacial tension, capillary force increases, which then facilitates imbibition [39]. However, a higher imbibition rate results in the earlier

Table 1: Results of imbibition experiments under different interfacial tensions with a salinity of 0 mg/L.

Interfacial tension [mN/m]	Time of stage I [min]	Imbibition height in stage I [mm]	Imbibition rate in stage I [mm/min]	Ultimate imbibition height [mm]
4.825	563	15.91	0.028	49.62
8.613	480	23.52	0.049	65.75
15.233	359	40.78	0.114	75.39
21.715	339	54.92	0.162	81.93
30.146	246	67.54	0.275	75.48

effect of gravity in the imbibition process, and an overall shorter Stage I. With the increase in interfacial tension, the ultimate imbibition height first increases and then decreases. The reason is that the increase in interfacial tension increases the capillary force which serves as the driving force, thus facilitating imbibition. However, the increasing imbibition rate causes the fluid to flow through the small pore throats instead of the large ones [40], thus increasing imbibition resistance. Furthermore, a higher imbibition rate results in the earlier effect of gravity on the imbibition process, and the imbibition height increases more slowly. Therefore, for a hydrophilic reservoir formation, there exists an optimal interfacial tension which allows the ultimate imbibition height to reach its maximum and represents the best case for displacing oil in the reservoir.

The overall results of the experiments with a salinity of 2500 mg/L are essentially the same as those with a salinity of 0 mg/L (Figure 3). With the increase in interfacial tension, the imbibition rate during stage I increases, and the ultimate imbibition height increases first and then decreases. The maximum is reached when the interfacial tension is 21.497 mN/m (0.005% TOF-1). Similarly, the experiments with salinities of 25000 mg/L and 70000 mg/L also show the same variation trend in imbibition, as shown in Figure 4. The ultimate imbibition height first increases and then decreases, and reaches its maximum when the interfacial tensions are 21.602 mN/m and 21.755 mN/m (0.005%TOF-1), respectively.

3.1.2. Variation in Imbibition Height of Rock Samples in Group B. In imbibition solutions with different TOF-1 volume fractions, the experimental results on the imbibition of rock samples in Group B are consistent with those in Group A, as shown in Table 2. With a salinity of 0–70000 mg/L and interfacial tension in the range of 4–30 mN/m, the duration of Stage I decreases with an increase in the interfacial tension. Moreover, the imbibition rate increases and the ultimate imbibition height first increases and then decreases.

Thus, for either hydrophilic rock samples or weakly-hydrophilic rock samples, there exists an optimal interfacial tension to achieve the maximum imbibition height, which represents the best imbibition effect. In these experiments, the imbibition solution with a TOF-1 volume fraction of 0.005% (with the interfacial tension of 21.497–21.755 mN/m) has the best imbibition effect.

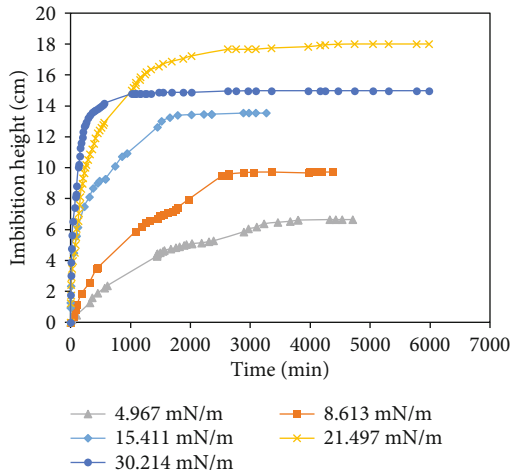

Figure 3: Change in imbibition height with time under different interfacial tensions with a salinity of 2500 mg/L.

According to the experimental results of the rock samples in Group A and Group B, the influence of the wettability of samples on imbibition height was further analyzed. The salinity of 2500 mg/L is taken as an example, as shown in Figure 5. During Stage I of imbibition, the growth rates of the imbibition height of hydrophilic and weakly hydrophilic samples both increase with the increase in interfacial tension, and under the same experimental conditions, the imbibition height of the hydrophilic samples increases more rapidly. The more hydrophilic rock samples show greater imbibition heights during both Stage I and Stage III. According to the analysis, a more hydrophilic rock sample results in a smaller wetting angle of the liquid-solid interface [41]. Also, a greater capillary force results in a faster increase in imbibition height and greater overall imbibition height.

3.2. Establishment of a Calculation Model for Imbibition Height. Flow resistance is an essential factor influencing the imbibition effect. However, the impact of flow resistance and the bending extent of pore throats are not adequately considered in the existing models. Thus, in this paper, a study was conducted to create a new imbibition model with consideration of flow resistance and the bending conditions of pore throats.

3.2.1. Model Establishment. Figure 6 shows a physical model for imbibition. The slender region in the middle is a capillary tube; the blue region is the imbibition solution; h denotes the imbibition height in the traditional capillary tube (Figure 6(a)); and h_s denotes the imbibition height in the improved model (Figure 6(b)). Considering the bending of pore throats, the capillary tube is curved, and the streamline of the imbibition solution is also a curve. In this paper, the fractal theory is used to describe the curved streamline.

The fractal theory describes the complexity and diversity of a research object through mathematical methods from the perspective of the fractal dimension. Due to self-similarity and iterative generation between the parts and the whole of the fractal body, there is a scaling relationship between the physical quantity $M(\varepsilon)$ to be studied and the measurement scale ε of the object, as follows [42]:

$$M(\varepsilon) \sim \varepsilon^{D_f}, \tag{4}$$

where D_f is the fractal dimension, which is an important parameter that describes the characteristics of a fractal body.

Stratigraphic rocks are also fractal [43]. Hence, the pore fractures and fluid streamlines in rocks present fractal distributions [44], with the scaling relationship as follows:

$$h_f = \varepsilon^{1\text{-}D_f} h_s^{D_f}, \tag{5}$$

where h_f denotes the imbibition length, with the unit of m; and h_s denotes imbibition distance, with the unit of m.

When the above scaling relationship is used to describe the fluid streamline in the stratum, ε denotes the equivalent pore diameter λ_c. Therefore, the scaling relationship can also be expressed as:

$$h_f = \lambda_c^{1\text{-}D_f} h_s^{D_f}, \tag{6}$$

D_f denotes the property parameter of the fractal body [45]:

$$D_f = d - \frac{\ln \varphi}{\ln (\lambda_{\min}/\lambda_{\max})}, \tag{7}$$

where d denotes spatial dimensions, with the constant of 2 or 3; φ denotes the porosity of the rock samples, dimensionless; $\lambda_{\max}$ and $\lambda_{\min}$ denote the maximum and minimum diameters of capillary tube, respectively, with a unit of m.

According to Figure 6(b), using the Bernoulli equation, the change in energy of the imbibition solution when moving from the initial position to the final position is:

$$p_1 + \frac{1}{2}\rho v_{f1}^{\ 2} + \rho g h_1 = p_2 + \frac{1}{2}\rho v_{f2}^{\ 2} + \rho g h_2 + \omega, \tag{8}$$

where P_1 and P_2 denote the pressures at the initial and final positions, respectively, with a unit of Pa; ρ is the density of the imbibition solution, with a unit of kg/m^3; v_{f1} and v_{f2} denote the flow velocities of imbibition solution at the initial and final positions, respectively, with a unit of m/s; h_1 and h_2 denote the heights of the initial and final positions, with a unit of m; and w denotes the pressure loss in the flow process of imbibition solution, with a unit of Pa.

The total energy loss of the fluid element in the imbibition process is:

$$E = 2\pi r \omega dr, \tag{9}$$

where r denotes the radius of the capillary tube, with a unit of mm.

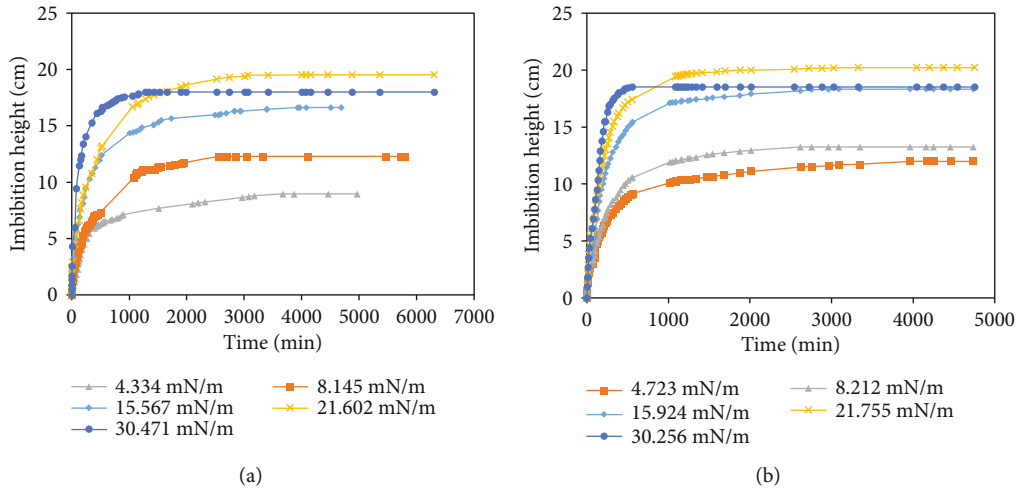

Figure 4: Change of imbibition height with time under different interfacial tensions. (a) With a salinity of 25000 mg/L. (b) With a salinity of 70000 mg/L.

Table 2: Results of imbibition experiments of rock samples in Group B.

Salinity (mg/L)	TOF-1 volume fraction [%]	Interfacial tension [mN/m]	Time of Stage I [min]	Imbibition height in Stage I [mm]	Imbibition rate in Stage I [mm/min]	Ultimate imbibition height [mm]
0	5	4.825	535	3.98	0.007	18.21
	0.5	8.613	462	15.07	0.033	19.92
	0.05	15.233	197	19.15	0.097	22.51
	0.005	21.715	175	19.46	0.111	24.03
	0.001	30.146	149	20.31	0.136	22.15
2500	5	4.967	492	12.75	0.026	21.15
	0.5	8.613	377	18.88	0.050	30.38
	0.05	15.411	170	22.64	0.133	43.15
	0.005	21.497	137	29.24	0.213	55.01
	0.001	30.214	125	30.15	0.241	35.07
25000	5	4.334	373	24.75	0.066	32.31
	0.5	8.145	353	25.36	0.072	44.48
	0.05	15.567	205	28.54	0.139	65.40
	0.005	21.602	127	35.75	0.281	80.59
	0.001	30.471	111	38.66	0.348	70.27
70000	5	4.723	347	33.99	0.098	84.23
	0.5	8.212	259	34.11	0.132	97.16
	0.05	15.924	223	88.94	0.399	135.28
	0.005	21.755	158	93.45	0.591	151.51
	0.001	30.256	105	95.92	0.914	148.78

The energy loss caused by internal friction in the imbibition process of the fluid element can be obtained through the formula for Newtonian internal friction:

$$W = -2\pi h_f \eta \frac{\mathrm{d}}{\mathrm{d}r}\left(r\frac{\mathrm{d}v_f}{\mathrm{d}r}\right), \tag{10}$$

where v_f denotes the flow velocity of the fluid in the axial direction of the capillary tube, with a unit of m/s; and η denotes the viscosity of imbibition solution, with a unit of Pa·s.

At the initial stage of imbibition, gravity has less effect on imbibition and is negligible. Therefore, the energy loss within the flow is caused by internal friction, that is, $E = W$.

$$2\pi r\omega \mathrm{d}r = -2\pi L_f \eta \frac{\mathrm{d}}{\mathrm{d}r}\left(r\frac{\mathrm{d}v_f}{\mathrm{d}r}\right). \tag{11}$$

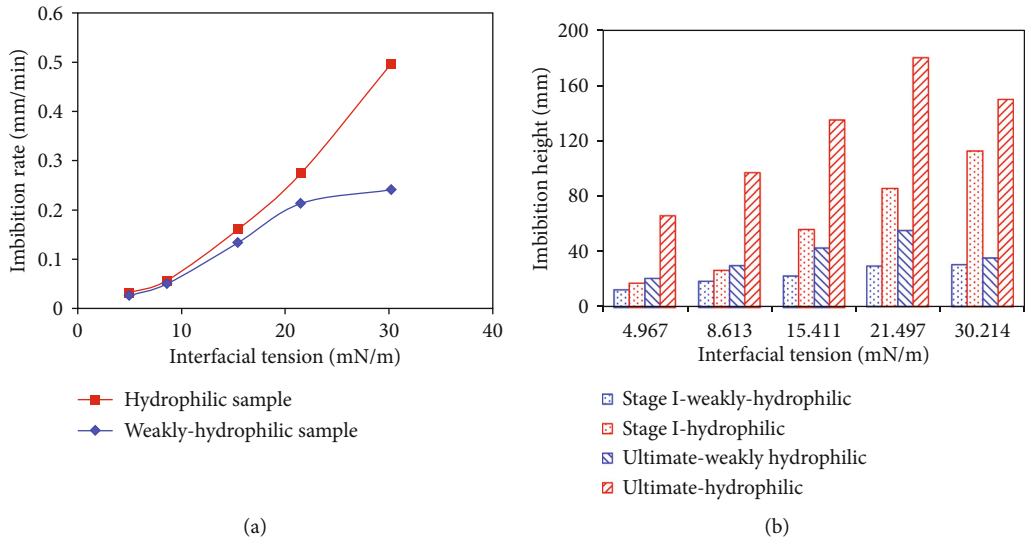

Figure 5: Effect of rock sample wettability on the imbibition rate and imbibition height. (a) Imbibition rate in Stage I. (b) Imbibition height.

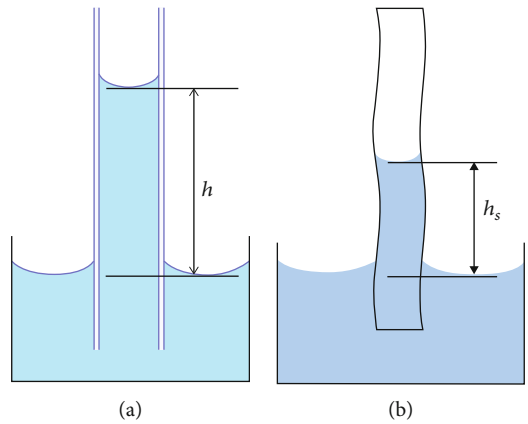

Figure 6: Imbibition models. (a) Traditional model. (b) New model.

Calculating the derivative of the imbibition height, the following equation can be obtained:

$$\frac{1}{\eta}\frac{\partial \omega}{\partial h_f} r \mathrm{d}r = -\frac{\mathrm{d}}{\mathrm{d}r}\left(r\frac{\mathrm{d}v_f}{\mathrm{d}r}\right), \tag{12}$$

where $\partial\omega/\partial h_f$ is the pressure gradient of the capillary tube along the direction of imbibition, with a unit of Pa/s.

The boundary condition can be expressed as:

$$\begin{cases} r = 0, \dfrac{\mathrm{d}v_f}{\mathrm{d}r} = 0 \\ r = r_c, v_f = 0 \end{cases}, \tag{13}$$

where r_c denotes the equivalent radius of the capillary tube, with the unit of m.

After integrating Equation (13) through the boundary condition, the following equation can be obtained:

$$v_f = \frac{1}{4\eta}\frac{\partial \omega}{\partial h_f}\left(r_c^2 - r^2\right). \tag{14}$$

The derivative of r can be obtained as:

$$\frac{\mathrm{d}v_f}{\mathrm{d}r} = -\frac{r}{2\eta}\frac{\partial \omega}{\partial h_f}. \tag{15}$$

Using the average imbibition rate as the equivalent value of the flow velocity of the fluid along the axial direction of the capillary tube, the following equation can be obtained:

$$\overline{v_{\mathrm{f}}} = \frac{1}{\pi r_c^2}\int_0^{r_c} 2\pi r v_f \mathrm{d}r = \frac{1}{\pi r_c^2}\int_0^{r_c} \frac{1}{4\eta}\frac{\partial \omega}{\partial h_f}\left(r_c^2 - r^2\right)2\pi r \mathrm{d}r = \frac{r_c^2}{8\eta}\frac{\partial \omega}{\partial h_f}. \tag{16}$$

Substituting Equation (16) into Equation (15), the following equation can be obtained:

$$\frac{\mathrm{d}v_f}{\mathrm{d}r} = -\frac{r}{2\eta} \cdot \frac{8\eta\overline{v_f}}{r_c^2} = -\frac{4r\overline{v_f}}{r_c^2}. \tag{17}$$

Substituting Equation (17) into the formula for Newtonian internal friction, the internal friction is calculated as follows:

$$\tau = \eta \frac{\mathrm{d}v_f}{\mathrm{d}r}\bigg|_{r=r_c} = -\eta \times \frac{4r_c\overline{v_f}}{r_c^2} = -\frac{4\overline{v_f}\eta}{r_c}. \tag{18}$$

Frictional force f (i.e., imbibition resistance) on the side of imbibition part of the capillary tube is calculated as:

$$f = 2\pi r_c h_f \tau = -8\pi\eta h_f \overline{v_f}. \tag{19}$$

The average imbibition rate $\overline{v_f}$ is:

$$\overline{v_f} = \frac{\mathrm{d}h_f}{\mathrm{d}t}. \tag{20}$$

Therefore, the differential equation for the length of the imbibition effect is:

$$\frac{\mathrm{d}}{\mathrm{d}t}\left(\pi r_c^2 \rho h_f \frac{\mathrm{d}h_f}{\mathrm{d}t}\right) = 2\pi\sigma r_c \cos\theta - 8\pi\eta h_f \frac{\mathrm{d}h_f}{\mathrm{d}t}, \tag{21}$$

where t denotes imbibition time, with the unit of s; σ denotes interfacial tension of imbibition solution, with the unit of N/m; and θ denotes wetting angle, with the unit of °.

After substituting Equation (6) into Equation (21), the formula for the change in imbibition height with time can be obtained by solving the equation:

$$h_s = \sqrt[2Df]{\frac{\sigma r_c \cos\theta}{\eta\lambda_c^{2-2D_f}}\left[t - \frac{r_c^2}{8\eta}\left(1 - \mathrm{e}^{-8\eta t/r_c^2\rho}\right)\right]}. \tag{22}$$

As the influence of gravity is not taken into consideration in the model derivation process, h_s denotes the height of Stage I (gravity is negligible).

3.2.2. Model Verification. The imbibition model was verified with the experimental data on the rock samples in Group A under different interfacial tensions, with a salinity of 0 mg/L taken as the example. The parameters of the imbibition solution and rock samples are shown in Table 3, and the calculation results are shown in Figure 7. By taking the imbibition resistance and the bending condition of the pore throats into account, the new model is able to obtain calculated results that fit well with the experimental results. The coefficient of determination (goodness of fit) R^2 was used to analyze the fitting effectiveness [46]. For solutions with the surface tensions of 4.825, 8.613, 15.233, 21.715, and 30.146 mN/m, the R^2 values are 0.909, 0.927, 0.965, 0.954 and 0.933, respectively, indicating that the proposed model can predict the imbibition trend in the initial period of imbibition. Overall, during Stage I, with the increase in imbibition time, the imbibition height rapidly increases while the imbibition rate gradually decreases. Also, at the same imbibition time, larger interfacial tension results in greater imbibition height.

Table 3: Basic parameters of cores and imbibition solution.

No.	R [μm]	D_f	ρ [kg/m^3]	σ [mN/m]	cos θ	η [mPa·a]
1				4.825	0.80	3.8
2				8.613	0.72	1.8
3	0.22	1.105	1000	15.233	0.68	1.5
4				21.715	0.63	1.3
5				30.146	0.55	1.1

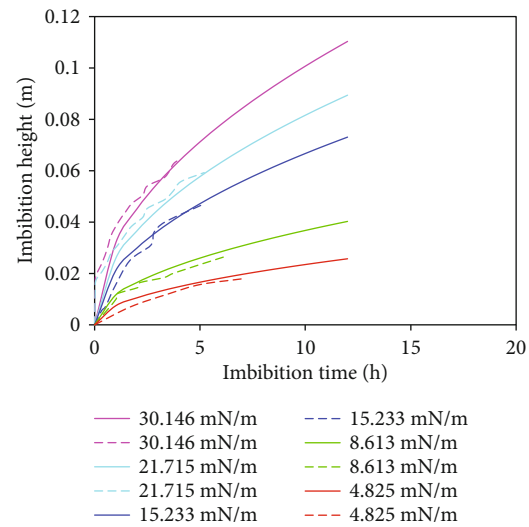

Figure 7: Comparison between the experimental results and calculation results obtained by the improved capillary model under different interfacial tensions. The dotted line indicates experimental results, and the solid line represents the calculated results.

4. Conclusions

In low-permeability reservoir formations, the increase in imbibition height with imbibition time can be divided into three stages. During Stage I, the capillary force, which serves as the driving force, plays a dominant role. The resistance of viscous force and gravity are negligible. Therefore, the imbibition height rapidly increases, followed by a slow increase. Interfacial tension has a significant effect on imbibition height. With the increase in interfacial tension, the imbibition rate during Stage I increases. The ultimate imbibition height first increases and then decreases, and the contribution of the imbibition height during the first stage to the ultimate imbibition height becomes greater. There is an optimal interfacial tension that allows the ultimate imbibition height to reach its maximum. The newly-established imbibition model takes into account the imbibition resistance and the bending of the pore throats, so it can reflect the change in imbibition height with time during Stage I. The calculation results are consistent with the experimental results, indicating

that the model is applicable for a low-permeability reservoir and would help predict the production results.

Data Availability

The data used to support the findings of this study are available from the first author upon request.

Conflicts of Interest

The authors declare that there are no conflicts of interest regarding the publication of this paper.

Acknowledgments

This work was supported by the Opening Fund of Shandong Key Laboratory of Oilfield Chemistry and the Fundamental Research Funds for the Central Universities.

References

[1] C. R. Clarkson, M. Freeman, L. He et al., "Characterization of tight gas reservoir pore structure using USANS/SANS and gas adsorption analysis," *Fuel*, vol. 95, pp. 371–385, 2012.

[2] P. Kathel and K. K. Mohanty, "Dynamic surfactant-aided imbibition in fractured oil-wet carbonates," *Journal of Petroleum Science and Engineering*, vol. 170, pp. 898–910, 2018.

[3] N. Pal, N. Kumar, R. K. Saw, and A. Mandal, "Gemini surfactant/polymer/silica stabilized oil-in-water nanoemulsions: design and physicochemical characterization for enhanced oil recovery," *Journal of Petroleum Science and Engineering*, vol. 183, article 106464, 2019.

[4] A. Javaheri, A. Habibi, H. Dehghanpour, and J. M. Wood, "Imbibition oil recovery from tight rocks with dual-wettability behavior," *Journal of Petroleum Science and Engineering*, vol. 167, pp. 180–191, 2018.

[5] Y. Liu, J. Cai, M. Sahimi, and C. Qin, "A study of the role of microfractures in counter-current spontaneous imbibition by lattice Boltzmann simulation," *Transport in Porous Media*, vol. 133, no. 2, pp. 313–332, 2020.

[6] J. Tu and J. J. Sheng, "Experimental and numerical study of surfactant solution spontaneous imbibition in shale oil reservoirs," *Journal of the Taiwan Institute of Chemical Engineers*, vol. 106, pp. 169–182, 2020.

[7] D. C. Standnes, L. A. D. Nogaret, H.-L. Chen, and T. Austad, "An evaluation of spontaneous imbibition of water into oil-wet carbonate reservoir cores using a nonionic and a cationic surfactant," *Energy & Fuels*, vol. 16, no. 6, pp. 1557–1564, 2002.

[8] A. J. Alshehri, E. Sagatov, and A. R. Kovscek, "Pore-Level Mechanics of Forced and Spontaneous Imbibition of Aqueous Surfactant Solutions in Fractured Porous Media," in *SPE Annual Technical Conference and Exhibition*, New Orleans, Louisiana, 2009.

[9] L. Sun, W. Pu, J. Xin, and Y. Wu, "Influence of surfactant on high temperature imbibition of low permeability cores," *Journal of China University of Petroleum*, vol. 36, no. 6, pp. 103–107, 2012.

[10] V. C. Santanna, T. N. C. Dantas, T. A. Borges, A. R. Bezerril, and A. E. G. Nascimento, "The influence of surfactant solution injection in oil recovery by spontaneous imbibition," *Petroleum Science and Technology*, vol. 32, no. 23, pp. 2896–2902, 2014.

[11] H. Alkan, M. Szabries, N. Dopffel et al., "Investigation of spontaneous imbibition induced by wettability alteration as a recovery mechanism in microbial enhanced oil recovery," *Journal of Petroleum Science and Engineering*, vol. 182, article 106163, 2019.

[12] T. Babadagli, "Analysis of Oil Recovery by Spontaneous Imbibition of Surfactant Solution," in *SPE International Improved Oil Recovery Conference in Asia Pacific*, Kuala Lumpur, Malaysia, 2003.

[13] J. O. Alvarez and D. S. Schechter, "Wettability alteration and spontaneous imbibition in unconventional liquid reservoirs by surfactant additives," *SPE Reservoir Evaluation & Engineering*, vol. 20, no. 1, pp. 107–117, 2017.

[14] A. Shen, Y. Liu, M. Bai et al., "Surfactant effects of wettability alteration and low IFT on countercurrent imbibition for tight oil formation," *Energy & Fuels*, vol. 32, no. 12, pp. 12365–12372, 2018.

[15] L. Gao, Z. Yang, and Y. Shi, "Experimental study on spontaneous imbibition chatacteristics of tight rocks," *Advances in Geo-Energy Research*, vol. 2, no. 3, pp. 292–304, 2018.

[16] J. Liu, J. J. Sheng, X. Wang, H. Ge, and E. Yao, "Experimental study of wettability alteration and spontaneous imbibition in Chinese shale oil reservoirs using anionic and nonionic surfactants," *Journal of Petroleum Science & Engineering*, vol. 175, pp. 624–633, 2019.

[17] I. W. R. Saputra, K. H. Park, F. Zhang, I. A. Adel, and D. S. Schechter, "Surfactant-assisted spontaneous imbibition to improve oil recovery on the Eagle Ford and Wolfcamp shale oil reservoir: laboratory to field analysis," *Energy & Fuels*, vol. 33, no. 8, pp. 6904–6920, 2019.

[18] J. Liu, J. J. Sheng, and W. Huang, "Experimental investigation of microscopic mechanisms of surfactant-enhanced spontaneous imbibition in shale cores," *Energy & Fuels*, vol. 33, no. 8, pp. 7188–7199, 2019.

[19] A. Kumar and A. Mandal, "Critical investigation of zwitterionic surfactant for enhanced oil recovery from both sandstone and carbonate reservoirs: adsorption, wettability alteration and imbibition studies," *Chemical Engineering Science*, vol. 209, article 115222, 2019.

[20] P. P. M. Keijzer and A. S. de Vries, "Imbibition of surfactant solutions," *SPE Advanced Technology Series*, vol. 1, no. 2, pp. 110–113, 1993.

[21] H. Tang, D. Lu, J. Xie, and Y. Zhang, "Experiment study ofwater imbibition injection for daanzai fracturing reservoir," *Journal of Southwest Petroleum Institute*, vol. 27, no. 2, pp. 41–44, 2005.

[22] E. W. Washburn, "The Dynamics of Capillary Flow," *Physical Review*, vol. 17, no. 3, pp. 273–283, 1921.

[23] J. Szekely, A. W. Neumann, and Y. K. Chuang, "The rate of capillary penetration and the applicability of the Washburn equation," *Journal of Colloid & Interface Science*, vol. 35, no. 2, pp. 273–278, 1971.

[24] B. V. Zhmud, F. Tiberg, and K. Hallstensson, "Dynamics of capillary rise," *Journal of Colloid & Interface Science*, vol. 228, no. 2, pp. 263–269, 2000.

[25] N. Fries and M. Dreyer, "An analytic solution of capillary rise restrained by gravity," *Journal of Colloid and Interface Science*, vol. 320, no. 1, pp. 259–263, 2008.

[26] C. Jian-Chao, Y. Bo-Ming, M. Mao-Fei, and L. Liang, "Capillary Rise in a Single Tortuous Capillary," *Chinese Physics Letters*, vol. 27, no. 5, article 054701, 2010.

[27] J. Cai and B. Yu, "A discussion of the effect of tortuosity on the capillary imbibition in porous media," *Transport in Porous Media*, vol. 89, no. 2, pp. 251–263, 2011.

[28] J. Cai, X. Hu, D. C. Standnes, and L. You, "An analytical model for spontaneous imbibition in fractal porous media including gravity," *Colloids and Surfaces A: Physicochemical and Engineering Aspects*, vol. 414, pp. 228–233, 2012.

[29] K. Li and H. Zhao, "Fractal prediction model of spontaneous imbibition rate," *Transport in Porous Media*, vol. 91, no. 2, pp. 363–376, 2012.

[30] P. O. Andersen, S. Evje, and H. Kleppe, "A model for spontaneous imbibition as a mechanism for oil recovery in fractured reservoirs," *Transport in Porous Media*, vol. 101, no. 2, pp. 299–331, 2014.

[31] J. Cai, E. Perfect, C. L. Cheng, and X. Hu, "Generalized modeling of spontaneous imbibition based on Hagen–Poiseuille flow in tortuous capillaries with variably shaped apertures," *Langmuir*, vol. 30, no. 18, pp. 5142–5151, 2014.

[32] P. O. Andersen, S. Evje, and A. Hiorth, "Modeling of spontaneous-imbibition experiments with porous disk—on the validity of exponential prediction," *SPE Journal*, vol. 22, no. 5, pp. 1326–1337, 2017.

[33] S. Ashraf and J. Phirani, "A generalized model for spontaneous imbibition in a horizontal, multi-layered porous medium," *Chemical Engineering Science*, vol. 209, article 115175, 2019.

[34] J. Xiao, Y. Luo, M. Niu et al., "Study of imbibition in various geometries using phase field method," *Capillarity*, vol. 2, no. 4, pp. 57–65, 2019.

[35] M. Meng, R. Zhong, and Z. Wei, "Prediction of methane adsorption in shale: classical models and machine learning based models," *Fuel*, vol. 278, article 118358, 2020.

[36] CPSC, "SY/T 5153-2017 Measurement of reservoir rock wettability," 2017.

[37] M. Meng and Z. Qiu, "Experiment study of mechanical properties and microstructures of bituminous coals influenced by supercritical carbon dioxide," *Fuel*, vol. 219, pp. 223–238, 2018.

[38] A. Li, *Petrophysics*, China university of Petroleum Press, Dongying, 2011.

[39] A. S. Zelenev and Z. Grenoble, "Wettability of reservoir rocks having different polarity by a model nonionic surfactant: fluid imbibition study into crushed rock packs," *Energy & Fuels*, vol. 32, no. 2, pp. 1340–1347, 2018.

[40] A. Kumar and A. Mandal, "Core-scale modelling and numerical simulation of zwitterionic surfactant flooding: designing of chemical slug for enhanced oil recovery," *Journal of Petroleum Science and Engineering*, vol. 192, article 107333, 2020.

[41] P. Pillai and A. Mandal, "Wettability modification and adsorption characteristics of imidazole-based ionic liquid on carbonate rock: implications for enhanced oil recovery," *Energy & Fuels*, vol. 33, no. 2, pp. 727–738, 2019.

[42] B. B. Mandelbrot, *The Fractal Geometry of Nature*, W. H. Freeman and Company, 1982.

[43] K. Liu, O. Mehdi, and L. Kong, "Fractal and multifractal characteristics of pore throats in the Bakken shale," *Transport in Porous Media*, vol. 126, no. 3, pp. 579–598, 2019.

[44] R. Guo, Q. Xie, X. Qu et al., "Fractal characteristics of pore-throat structure and permeability estimation of tight sandstone reservoirs: a case study of Chang 7 of the Upper Triassic Yanchang Formation in Longdong area, Ordos Basin, China," *Journal of Petroleum Science and Engineering*, vol. 184, article 106555, 2020.

[45] B. Yu and J. Li, "Some fractal characters of porous media," *Fractals*, vol. 9, no. 3, pp. 365–372, 2001.

[46] T. Tjur, "Coefficients of determination in logistic regression models—a new proposal: the coefficient of discrimination," *The American Statistician*, vol. 63, no. 4, pp. 366–372, 2009.